Reconstruction from Non-Uniform Spectral Data

Aditya Viswanathan[1] Anne Gelb[2] Douglas Cochran[1] Rosemary Renaut[2]

[1]School of Electrical, Computer & Energy Engineering
Arizona State University
{aditya.v,cochran}@asu.edu

[2]School of Mathematical & Statistical Sciences
Arizona State University
{anne.gelb,renaut}@asu.edu

Research supported in part by National Science Foundation grants
CNS 0324957, DMS 0510813 and DMS 0652833 (FRG).

SIAM Conference on Imaging Science
Chicago, USA

April 13 2010

Motivating Example

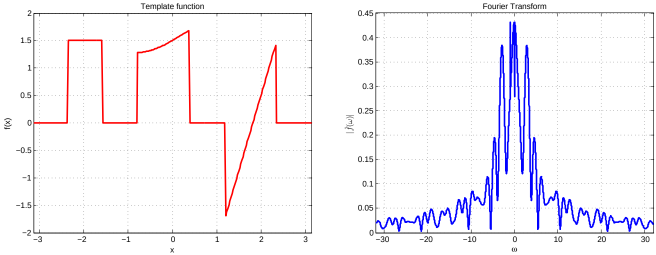

(a) Template Function (b) Fourier Transform

Figure: A motivating example

- Fourier samples violate the quadrature rule for discrete Fourier expansions.
- Computational issue – no FFT available
- How does variable sampling density affect reconstruction accuracy?

Motivating Example

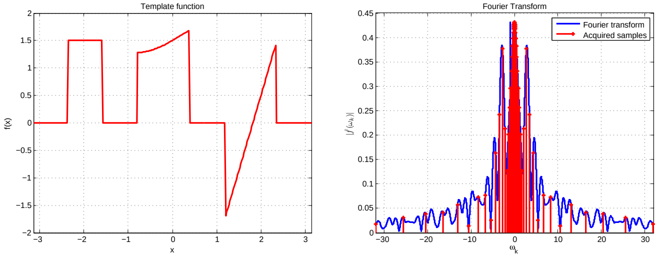

(a) Template Function (b) Fourier Coefficients, $N = 32$

Figure: A motivating example

- Fourier samples violate the quadrature rule for discrete Fourier expansions.
- Computational issue – no FFT available
- How does variable sampling density affect reconstruction accuracy?

Motivating Example

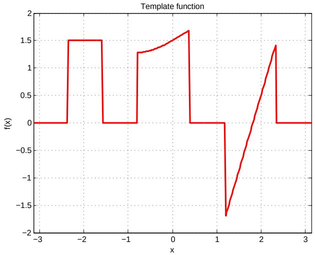

(a) Template Function

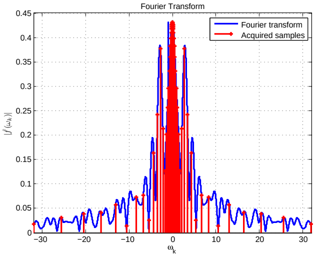

(b) Fourier Coefficients, $N = 32$

Figure: A motivating example

- Fourier samples violate the quadrature rule for discrete Fourier expansions.
- Computational issue – no FFT available
- How does variable sampling density affect reconstruction accuracy?

Application – Magnetic Resonance Imaging

Non-Cartesian sampling trajectories have some advantages

- greater resistance to aliasing and motion artifacts
- instrumentation concerns – ease in generating gradient waveforms

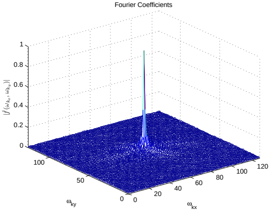

(a) Acquired Fourier Samples

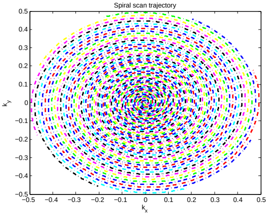

(b) Sampling Trajectory

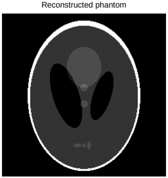

(c) Reconstructed Image

Figure: MR Imaging[a]

[a] Sampling pattern courtesy Dr. Jim Pipe, Barrow Neurological Institute, Phoenix, Arizona

In this Talk

We will discuss

- Issues with non-harmonic Fourier reconstruction
- Convolutional gridding
- Accuracy vs Sampling Density
- Spectral Re-projection methods

Outline

The Non-harmonic Reconstruction Kernel

Consider reconstruction using the sum

$$S_N \tilde{f}(x) = \sum_{|k| \le N} \hat{f}(\omega_k) e^{i\omega_k x}$$

We may write

$$S_N \tilde{f}(x) = (f * A_N)(x), \quad A_N(x) = \sum_{|k| \le N} e^{i\omega_k x}$$

where $A_N(x)$ is the non-harmonic kernel.

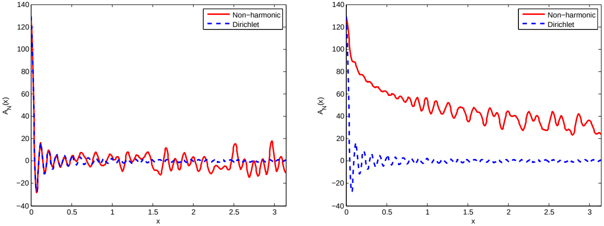

(a) Jittered Sampling (b) Log Sampling

Figure: $A_N(x), N = 64$

The Non-harmonic Reconstruction Kernel

Consider reconstruction using the sum

$$S_N \tilde{f}(x) = \sum_{|k| \leq N} \hat{f}(\omega_k) e^{i\omega_k x}$$

We may write

$$S_N \tilde{f}(x) = (f * A_N)(x), \quad A_N(x) = \sum_{|k| \leq N} e^{i\omega_k x}$$

where $A_N(x)$ is the non-harmonic kernel.

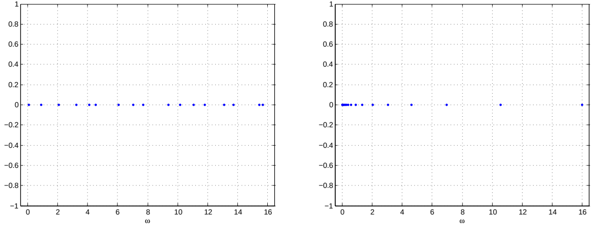

(a) Jittered Sampling (b) Log Sampling

Figure: Sampling Schemes

Reconstruction Examples

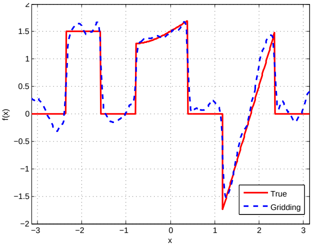

(a) “Jittered” Sampling

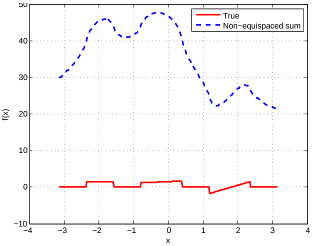

(b) “Log” Sampling

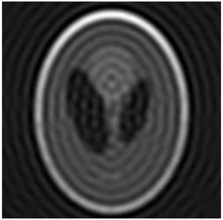

(c) “Spiral” Sampling

Figure: Non-harmonic Fourier sum Reconstruction, $N = 128$

Outline

Convolutional Gridding

Procedure:

1. Map the non-uniform modes to a uniform grid. A convolution operation is typically used.
2. Compute a Fourier or filtered Fourier partial sum.
3. If required, compensate for the mapping operation.

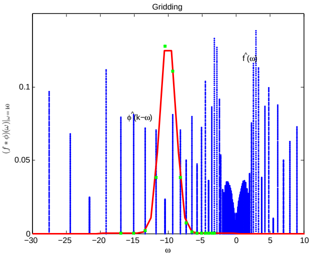

Figure: Gridding

The new coefficients on the uniform grid are therefore given by

$$\hat{f} * \hat{\phi}\Big|_{\omega=k} \approx \sum_{m \text{ st. } |k-\omega_m| \leq q} \alpha_m \hat{f}(\omega_m)\hat{\phi}(k-\omega_m)$$

Convolutional Gridding

Procedure:

1. Map the non-uniform modes to a uniform grid. A convolution operation is typically used.
2. Compute a Fourier or filtered Fourier partial sum.
3. If required, compensate for the mapping operation.

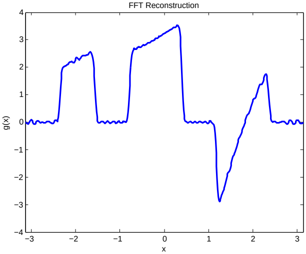

Figure: Fourier Reconstruction

The new coefficients on the uniform grid are therefore given by

$$\hat{f} * \hat{\phi}\Big|_{\omega=k} \approx \sum_{m \text{ st. } |k-\omega_m|\leq q} \alpha_m \hat{f}(\omega_m)\hat{\phi}(k-\omega_m)$$

Convolutional Gridding

Procedure:

1. Map the non-uniform modes to a uniform grid. A convolution operation is typically used.
2. Compute a Fourier or filtered Fourier partial sum.
3. If required, compensate for the mapping operation.

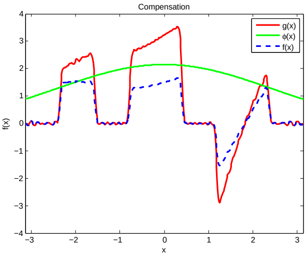

Figure: Compensation

The new coefficients on the uniform grid are therefore given by

$$\hat{f} * \hat{\phi}\Big|_{\omega=k} \approx \sum_{m \text{ st. } |k-\omega_m|\leq q} \alpha_m \hat{f}(\omega_m)\hat{\phi}(k-\omega_m)$$

Reconstruction Examples

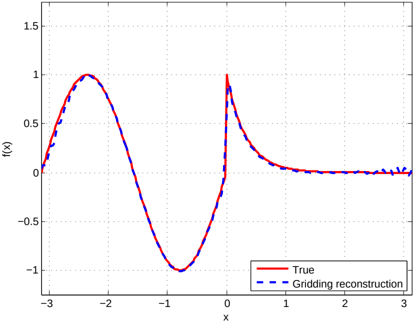

(a) Test Function reconstruction

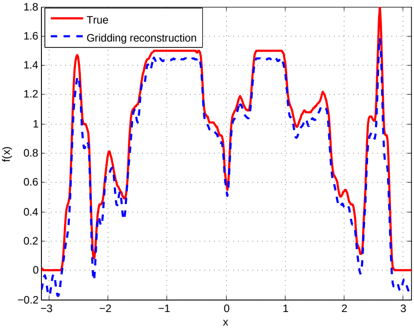

(b) Cross-section of a brain scan

Figure: Gridding reconstruction, $N = 128$ (processed by a 4^{th}-order exponential filter)

Gridding Error

Define the q-*vicinity* of k ($k \in \mathbb{Z}$) to be the set $\{\mathcal{P} = \omega : |k - \omega| \leq q,\ \omega, q \in \mathbb{R}, q > 0\}$.

Theorem (Convolutional Gridding Error)

Let $\hat{g} = \hat{f} * \hat{\phi}$ denote the true gridding coefficients and $\hat{\tilde{g}}$ denote the approximate gridding coefficients. Let Δ_k be the maximum distance between sampling points and $d_k := \frac{1}{\Delta_k}$ be the minimum sample density in the q-vicinity of k. Then, the gridding error at mode k is bounded by $|e(k)| = |\hat{g}(k) - \hat{\tilde{g}}(k)| =\leq C\frac{1}{d_k^2}$, $k = -N, ..., N$ for some positive constant C.

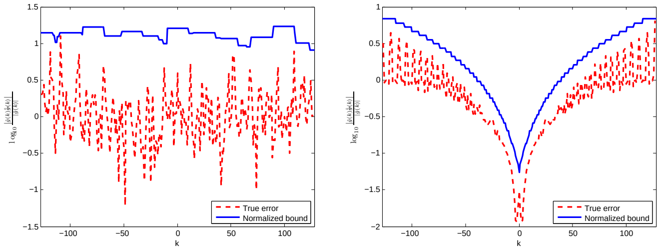

(a) Error bound, jittered sampling

(b) Error bound, log sampling

Figure: Error Plots

Gridding Error

Define the *q-vicinity* of k ($k \in \mathbb{Z}$) to be the set $\{\mathcal{P} = \omega : |k - \omega| \leq q,\ \omega, q \in \mathbb{R}, q > 0\}$.

Theorem (Convolutional Gridding Error)

Let $\hat{g} = \hat{f} * \hat{\phi}$ denote the true gridding coefficients and $\hat{\tilde{g}}$ denote the approximate gridding coefficients. Let Δ_k be the maximum distance between sampling points and $d_k := \frac{1}{\Delta_k}$ be the minimum sample density in the q-vicinity of k. Then, the gridding error at mode k is bounded by $|e(k)| = |\hat{g}(k) - \hat{\tilde{g}}(k)| =\leq C\frac{1}{d_k^2}$, $k = -N, ..., N$ for some positive constant C.

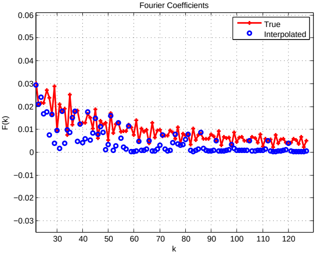

(a) Fourier coefficients – High modes

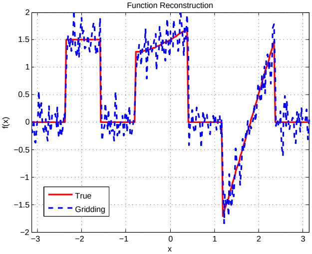

(b) Resulting reconstruction artifacts

Figure: Error Plots

Error vs Sampling Density

The reconstruction error is

$$e(x) \approx \sum_{|k|>N} \hat{g}(k)e^{ikx} + \sum_{|k|\leq N} \left(\hat{g}(k) - \hat{\tilde{g}}(k)\right) e^{ikx}$$

- 1^{st} term decreases as N increases (*standard Fourier truncation*)
- 2^{nd} term increases as N increases (*gridding error*)

  Gridding error $|S_N g(x) - S_N \tilde{g}(x)|$ can be shown to be bounded by $C \sum_{|k|\leq N} \frac{1}{d_k^2}$

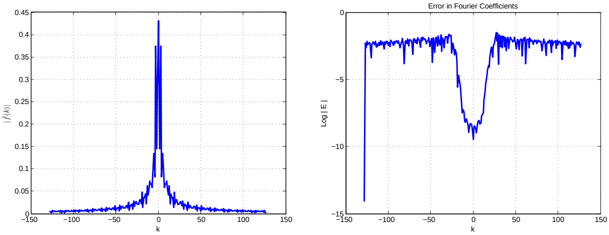

(a) Fourier coefficients (b) Coefficient error

Figure: Error in uniform re-sampling

While filtering decreases the error, the underlying problem is not solved.

Error vs Sampling Density

The reconstruction error is

$$e(x) \approx \sum_{|k|>N} \hat{g}(k)e^{ikx} + \sum_{|k|\leq N} \left(\hat{g}(k) - \hat{\tilde{g}}(k)\right) e^{ikx}$$

- 1^{st} term decreases as N increases (*standard Fourier truncation*)
- 2^{nd} term increases as N increases (*gridding error*)

  Gridding error $|S_N g(x) - S_N \tilde{g}(x)|$ can be shown to be bounded by $C \sum_{|k|\leq N} \frac{1}{d_k^2}$

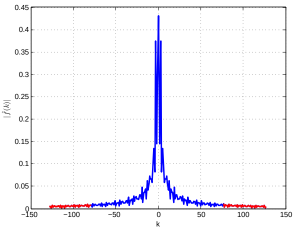

(a) Fourier coefficients

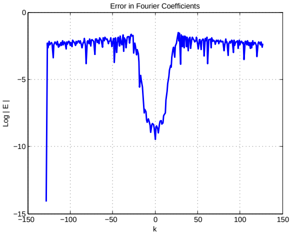

(b) Coefficient error

Figure: Error in uniform re-sampling

While filtering decreases the error, the underlying problem is not solved.

Error vs Sampling Density

The reconstruction error is

$$e(x) \approx \sum_{|k|>N} \hat{g}(k)e^{ikx} + \sum_{|k|\le N} \left(\hat{g}(k) - \hat{\tilde{g}}(k)\right) e^{ikx}$$

- 1^{st} term decreases as N increases (*standard Fourier truncation*)
- 2^{nd} term increases as N increases (*gridding error*)

Gridding error $|S_N g(x) - S_N \tilde{g}(x)|$ can be shown to be bounded by $C \sum_{|k|\le N} \frac{1}{d_k^2}$

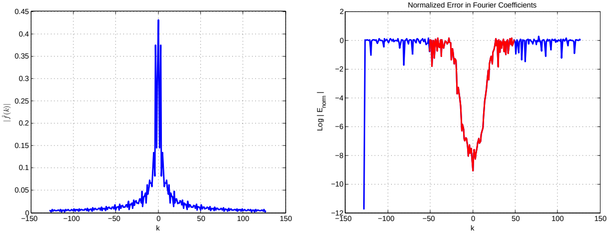

(a) Fourier coefficients (b) Coefficient error

Figure: Error in uniform re-sampling

While filtering decreases the error, the underlying problem is not solved.

Outline

Spectral Re-projection

- Spectral reprojection schemes were formulated to resolve the Gibbs phenomenon. They involve reconstructing the function using an alternate basis, Ψ (known as a Gibbs complementary basis).
- Reconstruction is performed using the rapidly converging series

$$f(x) \approx \sum_{l=0}^{m} c_l \psi_l(x), \quad \text{where} \quad c_l = \frac{\langle f_N, \psi_l \rangle_w}{\|\psi_l\|_w^2}, \; f_N \text{ is the Fourier expansion of } f$$

- Reconstruction is performed in each smooth interval. Hence, we require jump discontinuity locations
- High frequency modes of f have exponentially small contributions on the low modes in the new basis

Reducing the Impact of the High Mode Coefficients

- Using Gegenbauer polynomials, the re-projected expansion coefficients can be written as

$$\frac{1}{h_l^\lambda}\int_{-1}^{1}(1-\eta^2)^{\lambda-1/2}C_l^\lambda(\eta)\sum_{|k|\le N}\hat{\tilde{g}}(k)e^{i\pi k\eta}d\eta$$

- Damping of the high modes since

$$\frac{1}{h_l^\lambda}\int_{-1}^{1}(1-\eta^2)^{\lambda-1/2}C_l^\lambda(\eta)e^{i\pi k\eta}d\eta=\Gamma(\lambda)\left(\frac{2}{\pi k}\right)^\lambda i^l(l+\lambda)J_{l+\lambda}(\pi k)$$

- The gridding error can be shown to be

$$C'\cdot\rho(m,\lambda)\cdot\sum_{0<|k|\le N}\frac{1}{d_k^2}\left(\frac{1}{|k|}\right)^\lambda$$

Gegenbauer Reconstruction - Results

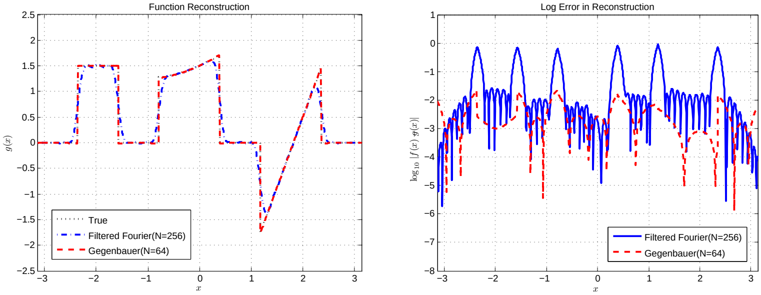

(a) Reconstruction (b) Reconstruction error

Figure: Gegenbauer reconstruction

- Filtered Fourier reconstruction uses 256 coefficients
- Gegenbauer reconstruction uses 64 coefficients
- Parameters in Gegenbauer Reconstruction - $m = 2, \lambda = 2$

Gegenbauer Reconstruction - Results

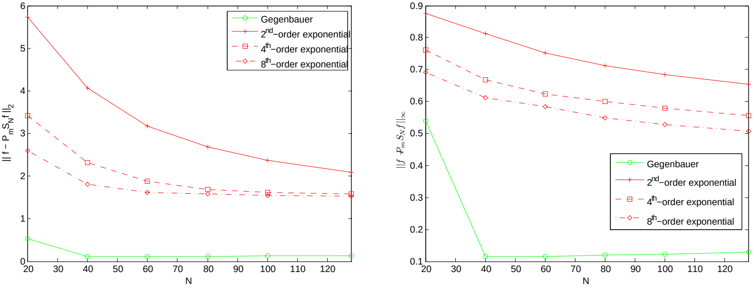

(a) 2-norm error   (b) Maximum-norm error

Figure: Error Plots – Filtered and Gegenbauer Reconstruction

- Filtered Fourier reconstruction uses 256 coefficients
- Gegenbauer reconstruction uses 64 coefficients
- Parameters in Gegenbauer Reconstruction - $m = 2, \lambda = 2$

Summary

- Fourier reconstruction from non-uniform spectral data is important in applications such as MR imaging.
- Families of non-harmonic exponentials do not usually constitute a basis for functions in $L^2(-\pi, \pi)$.
- The most popular reconstruction method is convolutional gridding, post-processed by low-pass filtering.
- Variable sampling density can result in poor reconstruction accuracy.
- Spectral re-projection methods can be useful in obtaining highly accurate reconstructions.

Current Emphasis

- Incorporating edge information into the reconstruction scheme .

References

- A. Viswanathan, A. Gelb, D. Cochran and R. Renaut, *On Reconstruction from Non-uniform Spectal Data*, Accepted to the Journal of Scientific Computing

Convolutional Gridding

- J. D. O'Sullivan, *Fast Sinc Function Gridding Algorithm for Fourier Inversion in Computer Tomography*, in IEEE Trans. Med. Imag., Vol. 4, 4 (1985).

Non-uniform FFTs

- J. A. Fessler and B. P. Sutton, *Nonuniform fast Fourier transforms using min-max interpolation*, in IEEE Trans. Signal Process., Vol. 51, 2 (2003), pp. 560–574.

Spectral Re-projection

- D. Gottlieb and C.W. Shu, *On the Gibbs phenomenon and its resolution*, in SIAM Review (1997), pp. 644–668.

Detecting Edges from Spectral Data

- A. Gelb and E. Tadmor, *Detection of Edges in Spectral Data*, in Appl. Comp. Harmonic Anal., 7 (1999), pp. 101–135.